

Parallel alignment of mold halves for UV-NIL process using loadcells

Paul Kastl¹, Zulfikar Wibowo¹, Dirk Oberschmidt¹

¹Berlin Institute of Technology, department of Micro and Precision Devices MFG, Germany

kastl@mfg.tu-berlin.de

Abstract

In UV-NIL thin-film replication of non planar surfaces, especially when using hard stamps, achieving precise alignment and gap adjustment between two mould halves is critical for achieving uniform gap width of a few microns. This paper presents a novel and easily implementable process to parallelize two planes which does not rely on soft stamps or passive compliant stages. An algorithm is presented which processes the signal of four symmetrically placed load cells in order to adjust the movement of an actuator. Once parallel, the gap width between the planes is easily adjustable as well. The use of load cells as robust and affordable sensors simplifies the implementation of the process. To validate the accuracy of this method, an autocollimation telescope was employed to measure the residual angular difference between the two planes after adjustment. The results demonstrate that the system achieves high accuracy in parallelization, providing a dependable solution for applications that require precise parallel alignment between two planes.

machine integrated metrology, parallelization, load cells, autocollimation telescope, angular measurement, plane alignment, gap adjustment

1. Introduction

Nanoimprint lithography with ultraviolet light (UV-NIL) is established as a process to quickly and efficiently produce nanoscale features down to 10 nm in resolution [1]. One of the numerous applications of these nanoscale features is the diffraction of light. Figure 1 depicts a typical UV-NIL process for pattern transfer in the replication of curved diffractive optical elements (cDOEs).

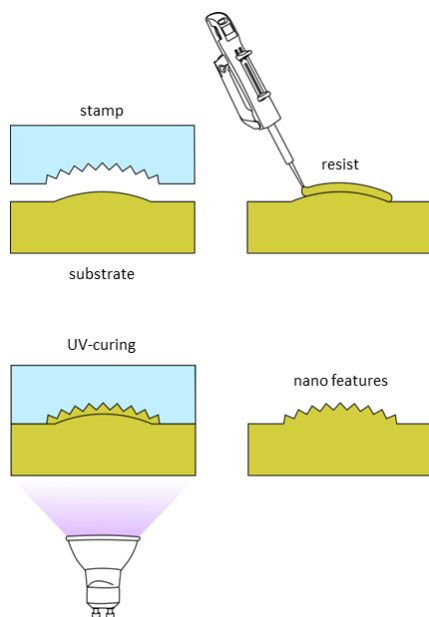


Figure 1: Exemplary UV-NIL process

The production of diffractive optical elements by means of machining is costly, due to high requirements for machine rigidity and temperature control. Holographic pattern generation in photo-curable resists is difficult to set up and inflexible when it comes to the adaptation of new geometries.

In the past UV-NIL prevailed as it offers high fidelity feature resolution and high throughput. It requires a master structure, which can either be mechanically or holographically produced. Based on that master structure a stamp is formed, which is then used to pattern a layer of UV-curable resist (Figure 2).

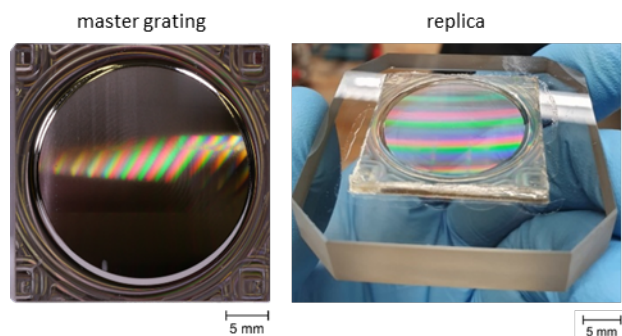


Figure 2: ultraprecision machined aluminum master grating and replica

Standardly, soft stamps made of Polydimethylsiloxane (PDMS) are used to ensure conformity of the stamp to the resist layer. However, hard stamps have been shown to facilitate even greater resolution [2]. To ensure conformity between a hard stamp and the resist layer, most often passive compliant stages are used. Soft stamps can distort, effectively limiting the achievable fidelity. Passive compliant stages are limited to a fixed pivot point in space for stage rotation which can lead to unwanted translational relative movement between stamp and substrate, causing defects in the nano patterns if centration is not good enough [3].

Soft stamps and passive compliant stages can be categorized as passive approaches for stamp alignment. As with multi-curved surfaces, these approaches are inadequate, and the quality of the results is particularly insufficient in the domain of curved diffractive optics. Curved DOEs offer diffraction and imaging capabilities in one element. This reduces the assembly and adjustment effort, the installation space and the number of

interfaces the light interacts with, thus increasing the efficiency of the optical set-up. Strongly curved DOEs (sDOEs) with radius of curvature down to 20 mm reduce assembly space even further. The department of Micro and Precision Devices (MFG) of the Berlin Institute of Technology (TUB) is capable of producing sDOEs by means of ultraprecision machining. Decreasing the cost of sDOEs by replicating them with UV-NIL is subject of current research.

This paper explores an active approach for aligning hard stamps to facilitate the replication of sDOEs. Hard stamps do not distort and the exclusion of a mechanical compliance mechanism in the stage to achieve alignment prevents unwanted translational relative movements between stamp and substrate. However, to overcome misalignment sensor feedback is necessary as with the active approach there is no compensating soft stamp or mechanical compliance mechanism.

Whereas with passive approaches little can be adjusted except stamping pressure, the active approach offers greater potential for tuning parameters to ensure high fidelity of replicated features. Sensor feedback is generated by four symmetrically placed load cells which measure the contact force between the stage and the hard stamp. The signals are evaluated in a programmable logic controller (PLC) and used to adjust the hexapod onto which the hard stamp is mounted. To measure the relative deviation from parallelism between the stamp and the stamping surface an autocollimator is used. The automated alignment is performed solely via the load cells, while the autocollimator is used only for the determination of the angular deviation from the parallel state. The smallest angular deviation from the parallel state achieved was $\Delta U = (8,0 \pm 1,2)$ arcsec and $\Delta V = (3,1 \pm 0,4)$ arcsec.

A phase correlation algorithm calculates the deviation of the autocollimator's reticle between the reference position, where the hard stamp is parallel with the stamping surface, and the final position of the hard stamp after each trial, measured in pixels.

By calibrating the autocollimator with an ultraprecision machine this pixel deviation is then transformed into an angle deviation in arcseconds. In the following the methodology for the trials will be explained in detail.

2. Methodology

2.1. Hardware

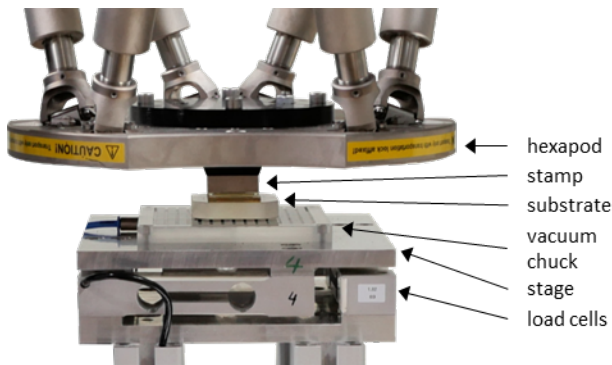


Figure 3: fine alignment stage of the replication machine

For the replication of strongly curved diffractive optical elements (sDOEs) a replication process was developed [4] and subsequently transferred to an industrial prototype [5] at the department of Micro and Precision Devices MFG of the Berlin Institute of Technology (TUB).

The system is equipped with a hexapod of Physik Instrumente (PI) SE & Co. KG, Karlsruhe, Germany for the fine alignment of

the stamp (Figure 3). Its repeatability is given with ± 0.5 arcsec for U and V and $\pm 0.1 \mu\text{m}$ in Z by the manufacturer.

The substrate clamped by a UV-transparent vacuum chuck, made of Polymethylmethacrylate (PMMA), which is mounted on the substrate stage equipped with four equidistantly placed load cells CP 5-3P1 of KERN & SOHN GmbH (former Sauter), Balingen-Frommern, Germany. Underneath the substrate stage is the UV-LED Unit FJ800 of PhoseonTechnology, Hillsboro, USA located. The stage assembly is mounted onto two servo-driven linear stages for coarse-alignment and to facilitate substrate handling. Additional hardware consists of a servo-driven linear stage to adjust the height of a dosing unit 1500XL from Nordson Corporation, Westlake, USA to apply resist to the substrate and the electrical equipment to power the actuators, sensors and PLC.

To measure the precision of the alignment method an autocollimator with focal length $f = 200$ mm was built from optical components of Thorlabs GmbH, Bergkirchen, Germany (according to [6]). The autocollimator measures the relative angular displacement of plane, reflective surfaces by collimating the diverging image of a reticle through a beamsplitter to infinity and then focusing the reflected light on a camera sensor. Any change in angular displacement of the reflective surface will lead to a displacement of the image of the reticle on the sensor (Figure 4).

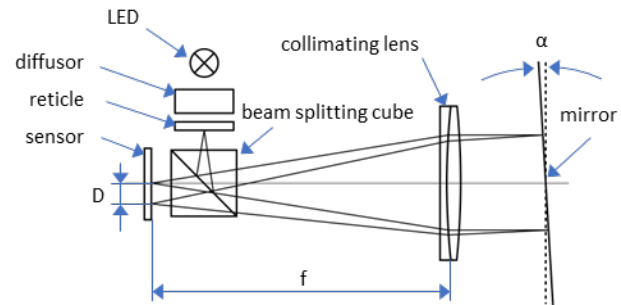


Figure 4: principle of an autocollimator

The displacement of the image of the reticle D is related to the angular displacement of the reflective surface α by the autocollimator formula [7]:

$$D = 2\alpha f \quad (1)$$

Calibration was done on tilting and rotating unit L8088 on a modified UP machine center MMC1100 by LT-Ultra Technology GmbH, Germany. The unit achieves angular positioning accuracy down to 3 arcseconds. To estimate the measurement uncertainty of the autocollimator, an uncertainty budget was compiled (Table 1, according to [8]).

Table 1: Uncertainty budget to estimate the measurement uncertainty of the autocollimator

Uncertainty source	Value	Type	Distribution	Divisor	std	Variance
unit	arcsec	-	-	-	arcsec	arcsec ²
tilting unit	3	B	rect.	$\sqrt{3}$	1,732	3
pixel size	1,1	A	rect	$2\sqrt{3}$	0,514	0,264
combined uncertainty sum					1,807	
uncertainty estimate					2	

By calculating the variance of the uncertainty values for the precision of the tilting and rotating unit and the pixel size of $3,45 \mu\text{m}$ of the sensor (by using equation (1)) and then taking the square root of their sum, the measurement uncertainty of the autocollimator is estimated to be 2 arcseconds.

To enable measurement with the autocollimator aluminium substitutes for stamp and substrate were ultraprecision machined by flycutting the reflective surfaces. The substitute substrate is fixed onto the stage and equipped with a 45° tilted mirror finish surface on one end.

The substitute stamp is mounted onto the hexapod. The collimated light rays emitted by the autocollimator are reflected upward (in negative Z-direction) by the chamfer surface and then again reflected by the stamp's surface. The returning rays are reflected again on the chamfer surface and then focused by the collimating lens onto the sensor (Figure 5).

Because of the double reflection on the chamfer surface a modified autocollimator equation for the angular displacement of the substitute stamp in V has to be used :

$$D_V = 4\alpha_V f \quad (2)$$

The autocollimator equation for the angular displacement of the substitute stamp in U remains unchanged.

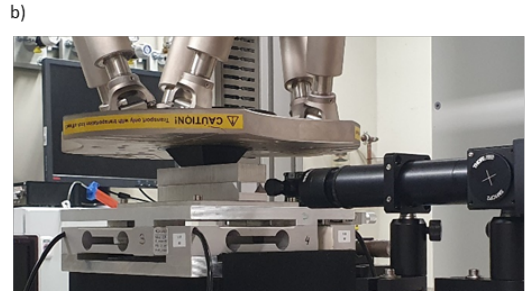
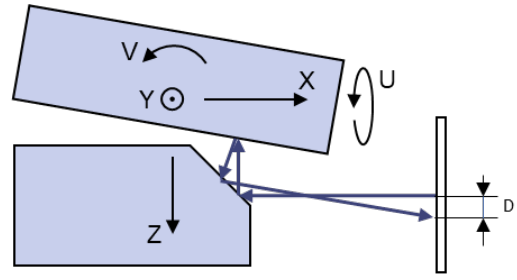


Figure 5: a) measurement principle with substitute bodies
b) laboratory set-up

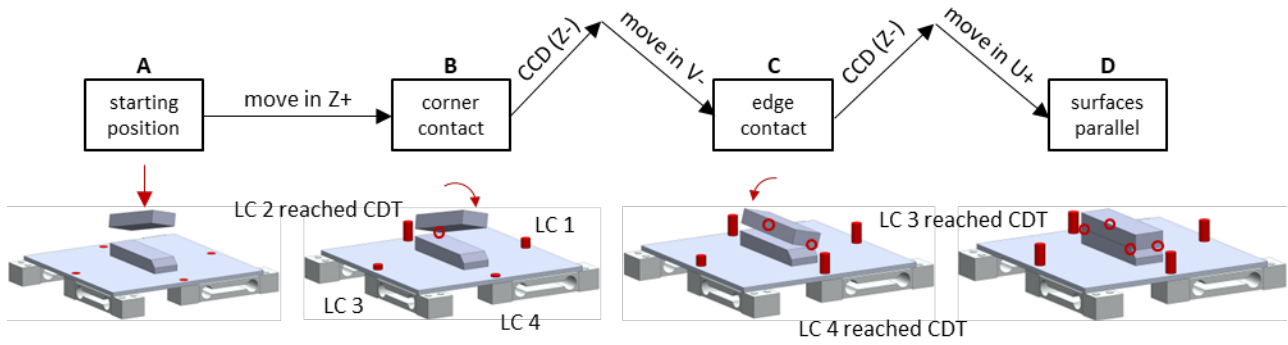


Figure 6: sequence of the alignment algorithm – the red columns indicate the load on each load cell

2.2. Sequence of experiments

In Figure 6 an exemplary sequence of the alignment is depicted. Lateral alignment was done manually once and the position saved for all trials.

To align stamp and substrate the stamp is positioned to an initial pose using the hexapod (A). From there it moves downwards, in positive Z-direction, with the translational velocity v_t . Surface contact is detected by one of the load cells exceeding the contact detection threshold CDT. The CDT is a variable parameter that can be set by the user. Is a contact detected, the hexapod is stopped. The corner of the contact is determined by evaluating the signals of the load cells. As is shown in state B of Figure 6 by the height of the red columns symbolizing the load cell signal, the contact corner is expected near the two highest detected loads. The pivot point for subsequent stamp movement is translated by the PLC to the contact corner.

After initial contact between the stamp and the substrate is detected via the load cells, a slight retraction in negative Z-direction is performed to account for the elastic deformation of the system and the braking distance of the hexapod. This retraction is referred to as the contact compensation distance (CCD).

After retraction, the hexapod is rotated in V-direction first. The direction depends on which side indicates the lesser load. In state C of Figure 6 it is load cell 4, so the rotation is performed in

direction V- with rotational velocity v_r , until load cell 4 exceeds the CDT again. Then, the rotation is stopped and another retraction is performed.

Once the retraction is completed, the rotation is repeated for U-direction, until load cell 3 exceeds the CDT again, as shown in state D of Figure 6. The alignment algorithm is now completed. After acquisition of a sensor image of the autocollimator, to measure the achieved precision of the alignment, the stamp is lastly positioned back to its initial pose to repeat alignment several times to examine the repeatability.

To obtain D in pixels of the acquired sensor image a phase correlation algorithm [9] is performed corresponding to a reference image representing a zero-position. The reference image was captured in advance, with the form and stamp placed in contact, ensuring they are perfectly parallel to each other.

To determine their influence on the alignment parameters CDT and CCD they were varied. The same initial pose was used for each trial. After setting one of the parameters to a certain value, the trial was repeated for that value from the same initial position a number of times. At first, the contact compensation distance is examined. Once an optimum was found, the contact detection threshold was varied.

3. Results

Figure 7 shows the angular deviation from a parallel alignment with respect to the CCD with CDT = 30 g. It can be

seen that for an increase in CCD the angular deviation decreases for both ΔU and ΔV , although the slope is greater for ΔU . With $CCD = 11 \mu m$ the angular deviation is smallest with $\Delta U = (8,0 \pm 1,2)$ arcsec and $\Delta V = (3,1 \pm 0,4)$ arcsec. This is equal to a height difference of $1 \mu m$ along the short edge of $30 mm$ and $1,5 \mu m$ along the long edge of $100 mm$ of the substitute stamp and substrate. To obtain the standard deviations the experiment for $CCD = 11 \mu m$ was repeated 30 times. The other data points ($CCD = 3, 4, 6, 9$) were repeated 3 times.

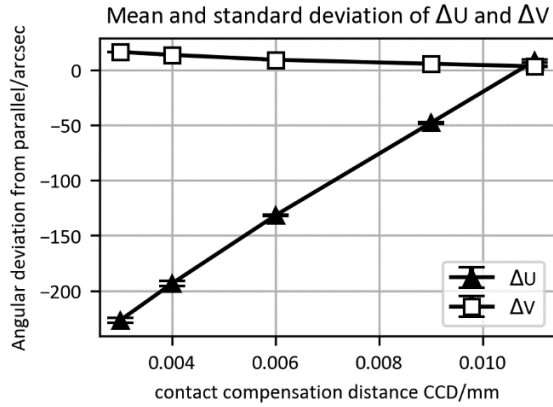


Figure 7: angular deviation from parallel with respect to the CCD

Figure 8 shows the angular deviation from parallel with respect to the CDT. For all data points the $CCD = 11 \mu m$ and the alignment was repeated 20 times (except for $CDT = 30 g$, where it was repeated 30 times). It can be seen that the CCD has an almost linear impact on ΔU while barely any impact on ΔV .

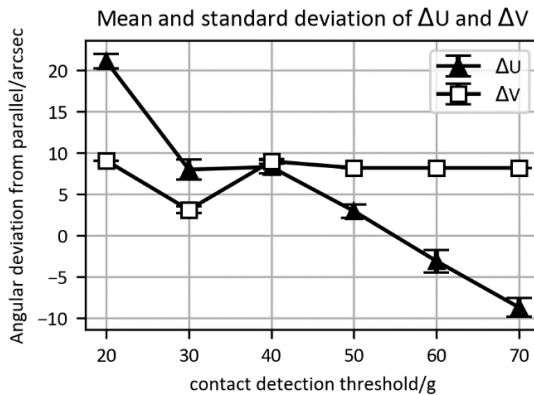


Figure 8: angular deviation from parallel with respect to the CDT

4. Discussion

The results indicate that it is possible to tune the parameters of the alignment algorithm to achieve parallelism between stamp and substrate within a few arcseconds of angular deviation. This qualifies the alignment method for implementation in NIL-processes for the replication of sDOEs.

Over all the conducted experiments ΔV has a smaller standard deviation than ΔU and is less impacted by the variation of either CCD or CDT . This can be explained by the larger dimension of stamp and substrate in X-direction, which corresponds to real optical components, in this case, reflective X-ray zone plates. The substrate is mounted centrally on the substrate stage, however its corners are not equidistant to the load cells, which results in different lengths of lever arms. In X-direction the lever arm is $50 mm$ long, in Y-direction $15 mm$. The same deflection will result in an increased load in X-direction. The CDT is thus reached much quicker and the difference in travel range of the

hexapod is less for any variation of parameters compared to the Y-direction. It is supposed that the alignment method achieves less angular deviation from parallelism the greater the surface to align is.

5. Conclusion

A novel method for parallel alignment of stamp and substrate in NIL has been developed and examined. It was shown that by the variation of CCD and CDT parallelism within a few arcseconds of angular deviation can be achieved. This qualifies the method as suitable for NIL. Its viability for NIL will be topic of further research.

It is of interest to examine the stability of the method in respect to the alteration of more variables. A comprehensive testing scheme has to be developed and undertaken to test the method for its robustness. Parameters like a change in the initial pose for otherwise the same parameters are closer to real world circumstances and should be examined.

In general the method rendered results which were close to what is confidently measurable with the autocollimator used. It is desirable to achieve greater resolution. For instance, this can be done by implementing a collimating lens with a focal length of $500 mm$ (see equation (1)).

6. Funding

We acknowledge the support this research has received from the Federal Ministry for Economic Affairs and Climate Action on the basis of a decision by the German Bundestag, the financial contribution of the "Investitionsbank Berlin" – IBB and the support of the project partners NOB Nano Optics Berlin GmbH and mrt micro resist technology GmbH.

References

- [1] S. Y. Chou and P. R. Krauss, 'Imprint lithography with sub-10 nm feature size and high throughput', *Microelectron. Eng.*, vol. 35, no. 1, pp. 237–240, Feb. 1997, doi: 10.1016/S0167-9317(96)00097-4.
- [2] B. Kwon and J. H. Kim, 'Importance of Molds for Nanoimprint Lithography: Hard, Soft, and Hybrid Molds', *J. Nanosci.*, vol. 2016, pp. 1–12, Jun. 2016, doi: 10.1155/2016/6571297.
- [3] H. Lan, Y. Ding, H. Liu, and B. Lu, 'Review of the wafer stage for nanoimprint lithography', *Microelectron. Eng.*, vol. 84, no. 4, pp. 684–688, Apr. 2007, doi: 10.1016/j.mee.2007.01.002.
- [4] S. Grützner *et al.*, 'Two-step replicated Nano Optical Pattern on curved Surfaces for Spectrometer Components', presented at the 47th international conference on Micro and Nano Engineering of the International Micro and Nano Engineering Society, Turin, 2021.
- [5] P. Kastl, C. Rödel, S. Kühne, J. Wolf, T. Krist, and D. Oberschmidt, 'A Method for the automated Replication of Diffractive Optical Elements with Strong Curvature', presented at the 49th international conference on Micro and Nano Engineering (MNE 2023), Berlin, Sep. 26, 2023.
- [6] B. Patton, 'Using an autocollimator to align 4f systems'. Accessed: Oct. 16, 2024. [Online]. Available: <https://focalplane.biologists.com/2022/06/29/using-an-autocollimator-to-align-4f-systems/>
- [7] J. Yuan and X. Long, 'CCD-area-based autocollimator for precision small-angle measurement', *Rev. Sci. Instrum.*, vol. 74, no. 3, pp. 1362–1365, Mar. 2003, doi: 10.1063/1.1539896.
- [8] T. Adams, 'Guide for the Estimation of Measurement Uncertainty In Testing', A2LA, Guide, Jul. 2002. Accessed: Aug. 16, 2024. [Online]. Available: http://www.sadcmnet.org/SADCWaterLab/Archived_Reports/2006%20Reports%20and%20Docs/A2LA_est.pdf
- [9] C. D. Kuglin, 'The phase correlation image alignment method', *IEEE Int Conf Cybern. Soc.* 1975, pp. 163–165, 1975.